Eidgenössische Technische Hochschule Zürich

Ecole polytechnique fédérale de Zurich
Politecnico federale di Zurigo
Swiss Federal Institute of Technology Zurich

Long-Term Evolution of Coorbital Motion

J. Waldvogel

Research Report No. 98-05
May 1998

Seminar für Angewandte Mathematik
Eidgenössische Technische Hochschule
CH-8092 Zürich
Switzerland

Long-Term Evolution of Coorbital Motion

J. Waldvogel

Seminar für Angewandte Mathematik
Eidgenössische Technische Hochschule
CH-8092 Zürich
Switzerland

Research Report No. 98-05 May 1998

Abstract

In these lectures the planar problem of three bodies with masses m_0, m_1, m_2 will be used as a model of coorbital motion, thus leaving the analysis of three-dimensional effects to later work. For theoretical as well as for numerical studies the choice of appropriate variables is essential. Here Jacobian coordinates and a rotating frame of reference will be used. The application of the Hamiltonian formalism in connection with complex notation will greatly simplify the differential equations of motion.

The results obtained are partially of experimental nature, based on reliable numerical integration. Obviously, chaos plays an important role. An orderly behaviour occurs for small mass ratios $\epsilon := (m_1 + m_2)/m_0$; however, the typical phenomena persist even for mass ratios as large as 0.01. In particular, proper coorbital motion seems to be chaotic, but stable for very long periods of time. The interaction of the satellites, as they approach each other, is qualitatively described by Hill's lunar problem. Temporary capture between independently revolving satellites is delicate and can only happen when close encounters are involved. It seems to be able to persist for very long times, though, even for mass ratios as large as $\epsilon = 0.1$.

1 Introduction

Coorbital motion is a particular case of three-body motion: the motion of two small satellites about a central body. For simplicity, only the planar case will be considered. Although coorbital motion constitutes a simplified model of three-body motion it displays surprisingly complex dynamics. In earlier work mainly a single close encounter in the motion of satellites in close circular orbits was considered, see, e.g. [4, 9].

In this study the succession of many close encounters is considered. Dermott and Murray [2] observed that coorbital motion may eventually decay, and they gave an estimate of the lifetime. The basic situation consists of a large central planet m_0 and two small satellites m_1, m_2 revolving about m_0 in the same plane.

Pairs of small satellites revolving about a central planet are called coorbital if their orbits are close in an appropriate sense. Three types of motion may be distinguished, all of which actually occur in the Saturnian ring system: (1) one-to-tone resonance or *proper coorbital motion*, such as the motion of Janus and Epimetheus, (2) *stable revolution*, such as the motion of the F ring shepherds Pandora and Prometheus, (3) *temporary capture*, such as the motion of two neighbouring ring particles who remain in bound state for an extended period of time.

In order to handle the long-term evolution of coorbital motion it is important to use appropriate coordinates. For describing a single close encounter coordinates which lead to Hill's lunar problem in the limiting case of small satellite masses seem to be appropriate [9]. Therefore we will basically introduce Hill's coordinates; however, the time intervals of weakly perturbed Kepler motion between close encounters will have to be considered as well.

Since we restrict ourselves to the planar case we will use complex notation for convenience. First, we will collect the tools of complex notation, complex gradients and canonical transformations. Jacobian coordinates and Levi-Civita regularization will be summarized for later use.

Then, the behaviour at a single close encounter will be summarized, following earlier work by Hénon and Petit [4, 6], and by Spirig and Waldvogel [9, 12]. Various coordinate systems with the above mentioned properties will be used with the goal of adequately describing coorbital motion. Numerical experiments suggest that coorbital pairs of type (1) have a finite lifetime that can be very long for small mass ratios and favourable initial conditions.

2 Tools

2.1 Complex Notation

For discussing the planar three-body problem we use the Hamiltonian formalism and complex notation. The basic equations will be collected together with the notation to be used.

Let $\vec{z} = (x, y)^T$ be the Cartesian coordinates of a point mass, and introduce the

complex coordinate z and its conjugate $\bar{z}$ according to

$$z = x + iy \in \mathbb{C}, \quad \bar{z} = x - iy, \quad i = \sqrt{-1} \; . \tag{1}$$

Consider the function $H(x, y)$, e.g. a Hamiltonian with the dependence on the momenta suppressed, and write it in terms of z and $\bar{z}$,

$$H(x, y) = \widetilde{H}(z, \bar{z}) \; . \tag{2}$$

Then the complex gradient

$$\mathrm{grd}\, H := \frac{\partial H}{\partial x} + i \, \frac{\partial H}{\partial y} \tag{3}$$

becomes

$$\mathrm{grd}\, H := 2 \, \frac{\partial \widetilde{H}}{\partial \bar{z}} \; , \tag{4}$$

as is seen by differentiating (2) by means of (1).

Next, we consider a Hamiltonian depending on several complex coordinates $z_k \, (k = 1, \ldots, N)$, their canonically conjugated momenta p_k, and the corresponding complex conjugated variables $\bar{z}_k$, $\bar{p}_k$ $(k = 1, \ldots, N)$. The typical transformation of variables to be considered is a conformal map in each coordinate. Therefore, with $Z_k, P_k \, (k = 1, \ldots, N)$ being the new coordinates and momenta, we define the coordinate transformation by the functions

$$z_k = z_k(Z_1, Z_2, \ldots, Z_N), \; k = 1, \ldots, N \; , \tag{5}$$

analytic in every variable, and we are looking for the definition of the canonically conjugated momenta P_k. Using the well-known technique of the generating function (see, e.g. [8]) we proceed as follows. From the generating function

$$W(Z_k, p_k) := Re \, \sum_{k=1}^{N} \, z_k(Z) \cdot \bar{p}_k \tag{6}$$

the new momenta are obtained as the partial derivatives of W with respect to the new coordinates, in complex notation:

$$P_k = 2 \, \frac{\partial W}{\partial \overline{Z}_k} \; , \quad k = 1, \ldots, N \; . \tag{7}$$

2.2 The Hamiltonian

The technique discussed in the previous section conveniently allows to set up the equations of motion in various coordinate systems. Consider now the three point masses m_0, m_1, m_2 at the inertial positions $x_0, x_1, x_2 \in \mathbb{C}$, respectively, with the center of mass at rest, $\Sigma \, m_j \, x_j = 0$. We will formulate the equations of motion in terms of the relative coordinates with respect to x_0,

$$z_1 := x_1 - x_0, \quad z_2 := x_2 - x_0 \; . \tag{8}$$

The position x_0 of the reference body m_0, in turn, may be recovered from

$$(m_0 + m_1 + m_2)\, x_0 = -m_1\, z_1 - m_2\, z_2 \ .$$

It is easily seen that the canonically conjugated momenta in complex notation are

$$p_j = m_j\, \frac{dx_j}{dt} \ , \quad j = 1, 2, \ .$$

The Hamiltonian H and angular momentum C of the planar three-body problem are then given by

$$\begin{aligned} H &= \frac{|p_1 + p_2|^2}{2m_0} + \frac{|p_1|^2}{2m_1} + \frac{|p_2|^2}{2m_2} - \frac{m_0\, m_1}{|z_1|} - \frac{m_0\, m_2}{|z_2|} - \frac{m_1\, m_2}{|z_2 - z_1|} \ , \\ C &= Im(\bar{z}_1\, p_1 + \bar{z}_2\, p_2) \ . \end{aligned} \tag{9}$$

In this study we will consider coorbital configurations with m_0 as the central body and m_1, m_2 as the possibly interacting satellites. Therefore, it is useful to introduce Jacobi coordinates R, D with respect to m_0 and the center of mass of m_1 and m_2:

$$R = \mu_1\, z_1 + \mu_2\, z_2, \quad D = z_2 - z_1 \ , \tag{10}$$

where

$$\mu_j = \frac{m_j}{m_1 + m_2} \ , \quad j = 1, 2 \tag{11}$$

are the relative masses of the satellites. This yields the transformation

$$z_1 = z_1(R, D) = R - \mu_2\, D, \quad z_2 = z_2(R, D) = R + \mu_1\, D \ . \tag{12}$$

With the generating function according to (6),

$$W(R, D, p_1, p_2) = Re\Big(z_1(R, D)\, \bar{p}_1 + z_2(R, D)\, \bar{p}_2\Big) \ ,$$

we obtain the definition of the canonically conjugated momenta P_R, P_D from Equ. (7):

$$\begin{aligned} P_R &= 2\, \frac{\partial W}{\partial \overline{R}} = p_1 + p_2 \\ P_D &= 2\, \frac{\partial W}{\partial \overline{D}} = \mu_1\, p_2 - \mu_2\, p_1 \ . \end{aligned}$$

Solving this for the old momenta yields

$$p_1 = \mu_1\, P_R - P_D, \ p_2 = \mu_2\, P_R + P_D \ , \tag{13}$$

and the Hamiltonian and angular momentum (9) become

$$\begin{aligned} H &= \frac{|P_R|^2}{2m_0} + \frac{|\mu_1\, P_R - P_D|^2}{2m_1} + \frac{|\mu_2\, P_R + P_D|^2}{2m_2} \\ &\quad - \frac{m_0\, m_1}{|R - \mu_2\, D|} - \frac{m_0\, m_2}{|R + \mu_1\, D|} - \frac{m_1\, m_2}{|D|}\ , \\ C &= Im(\overline{R}\, P_R + \overline{D}\, P_D)\ . \end{aligned} \tag{14}$$

2.3 Regularization

Since repeated close encounters of m_1 and m_2 are involved in coorbital motion it may be necessary to regularize the respective binary collisions. A review of Levi-Civita's regularizing transformation [5], written in complex notation, is given in this section.

(i) A single binary collision between a particle at position z with momentum p and a central body at the origin is regularized by introducing new coordinates and momenta Z, P according to Levi-Civita's conformal canonical transformation

$$z = Z^2, \quad p = \frac{P}{2\overline{Z}}\ . \tag{15}$$

The second equation follows from (7) with the generating function $W = \frac{1}{2}\,(Z^2\bar{p} + \bar{Z}^2 p)$. Regularization is achieved by introducing the fictitious time s and the new Hamiltonian K according to

$$\begin{aligned} dt &= r \cdot ds, \quad r = |z| = |Z|^2 \\ K &= r(H - h)\ , \end{aligned} \tag{16}$$

where h is the fixed value of H on the orbit under consideration.

(ii) Hill's lunar problem has a special significance for coorbital motion, see Section 3. It approximates coorbital motion in a rotating (and pulsating) coordinate system during the close encounters of the satellites [9]. The model is given by the Hamiltonian [12]

$$H = \frac{1}{2}\,|p|^2 + Im(\bar{p}\, z) - \frac{3}{8}\,(z^2 + \bar{z}^2) - \frac{1}{4}\,z\bar{z} - \frac{1}{|z|}\ . \tag{17}$$

Using the transformations (15), (16) yields the new Hamiltonian

$$K = \frac{P\,\bar{P}}{8} + |Z|^2\left(\frac{1}{2}\,Im(\bar{P}Z) - \frac{3}{8}\,(Z^4 + \bar{Z}^4) - \frac{1}{4}\,Z^2\,\bar{Z}^2 - h\right) - 1\ , \tag{18}$$

a polynomial of degree 2 in P and 6 in Z. For completeness the equations of motion are given here:

$$\frac{dZ}{ds} = 2\,\frac{\partial K}{\partial \bar{P}}\ , \quad \frac{dP}{ds} = -2\,\frac{\partial K}{\partial \bar{Z}}\ , \quad \frac{dt}{ds} = Z\overline{Z}\ .$$

(iii) As a by-product, we mention the possibility of simultaneously regularizing all binary collisions in the planar three-body problem [11]. The goal is to introduce *two* new complex

coordinates Z_1, Z_2 such that the three complex relative positions $z_1, z_2, z_2 - z_1$ appear as complete squares, $z_1 = \zeta_1^2$, $z_2 = \zeta_2^2$, $z_2 - z_1 = \zeta_0^2$. Since this implies

$$\zeta_2^2 = \zeta_0^2 + \zeta_1^2 \ , \tag{19}$$

it suffices to parameterize the relation (19) (formally Pythagoras' theorem) by 2 new variables Z_1, Z_2. We choose the well-known relations using quadratic polynomials for ζ_1, ζ_2,

$$z_1 = \Big(\frac{Z_1^2 - Z_2^2}{2}\Big)^2, \quad z_2 = \Big(\frac{Z_1^2 + Z_2^2}{2}\Big)^2, \quad z_2 - z_1 = Z_1^2\, Z_2^2 \ .$$

Equ. (7), together with the generating function

$$W = \frac{1}{2}\,(z_1\,\bar{p}_1 + \bar{z}_1\,p_1 + z_2\,\bar{p}_2 + \bar{z}_2\,p_2)$$

provides the definition of the conjugated momenta:

$$\begin{pmatrix} P_1 \\ P_2 \end{pmatrix} = \begin{pmatrix} \overline{Z}_1 & \overline{Z}_1 \\ -\overline{Z}_2 & \overline{Z}_2 \end{pmatrix} \begin{pmatrix} (\overline{Z}_1^2 - \overline{Z}_2^2)\,p_1 \\ (\overline{Z}_1^2 + \overline{Z}_2^2)\,p_2 \end{pmatrix} \ .$$

Solving for p_1, p_2 yields

$$\begin{aligned} p_1 &= \frac{\overline{Z}_2\,P_1 - \overline{Z}_1\,P_2}{2\,\overline{Z}_1\,\overline{Z}_2(\overline{Z}_1^2 - \overline{Z}_2^2)} \\ p_2 &= \frac{\overline{Z}_2\,P_1 + \overline{Z}_1\,P_2}{2\,\overline{Z}_1\,\overline{Z}_2(\overline{Z}_1^2 + \overline{Z}_2^2)} \ . \end{aligned}$$

Finally, the time transformation

$$dt = r_0\,r_1\,r_2 \cdot ds, \quad r_j = |z_j|$$

transforms the Hamiltonian (9) into the regularized

$$K = K(Z_1, Z_2, P_1, P_2) = r_0\,r_1\,r_2(H - h) \ ,$$

which turns out to be a polynomial of degree 2 in P, and of degree 12 in Z. A recent account of implementing this regularization is given in [3].

3 A Single Close Encounter

We restrict ourselves to summarizing results obtained with the circular model described in [9]. Approximative data from two known coorbital pairs in the Saturnian ring system will be given.

Let

$$\epsilon := (m_1 + m_2)/m_0 << 1 \tag{20}$$

be the ratio of the total satellite mass $m_1 + m_2$ and the central mass m_0, and assume the satellites m_1, m_2 to initially move on nearly identical circles of radii R_1, R_2, respectively, about m_0. Following the definitions in Equ. (10) we introduce

$$R_{12} := \mu_1 R_1 + \mu_2 R_2, \quad \Delta := |R_2 - R_1| \tag{21}$$

as the "mean" orbital radius (more precisely, the orbital radius of the satellites' common center of mass at a close encounter) and the orbital separation.

Furthermore, we introduce the relative separation

$$\delta := \Delta / R_{12} \tag{22}$$

and the impact parameter

$$c := \delta \cdot \epsilon^{-1/3} \ . \tag{23}$$

In [9] it is established that during a close encounter of the satellites coorbital motion behaves like a particular solution of Hill's lunar problem. This is seen by using Jacobi coordinates R, D according to (10) and introducing scaled rotating and pulsating coordinates z according to

$$D = \epsilon^{1/3} R z, \quad z = x + iy \ . \tag{24}$$

If the coorbital configuration is near-circular, i.e. if

$$R = R_0 \, e^{i\omega t} \ \text{ with } \ \omega^2 R_0^3 = m_0 \ ,$$

then the limit $\epsilon \to 0$ results in Hill's lunar equations

$$\begin{aligned} \ddot{x} - 2\dot{y} - 3x \ &+ \ x/r^3 \ = \ 0, \ r = \sqrt{x^2 + y^2} \\ \ddot{y} + 2\dot{x} \qquad &+ \ y/r^3 \ = \ 0 \end{aligned} \tag{25}$$

with the energy integral

$$\frac{1}{2} \, (\dot{x}^2 + \dot{y}^2) - \frac{3}{2} \, x^2 - \frac{1}{r} = h \ . \tag{26}$$

As a consequence of the definition (23), a single close encounter is described by the uniquely determined orbit satisfying Hill's lunar equations (25) and

$$\lim_{t \to -\infty} \ x(t) = c > 0 \ . \tag{27}$$

The main result on circular coorbital motion is based on the limiting case $c \to 0$. Introducing scaled coordinates

$$\xi = c^{-1} x, \quad \eta = c^2 y, \quad \tau = c^3 t \tag{28}$$

into (25), (26) yields in zeroth order

$$\begin{aligned} -\,2\eta' \;-\,3\xi \;&=\; 0 \\ \eta'' \,+\,2\xi' \;+\,\frac{1}{\eta|\eta|} \;&=\; 0 \\ \frac{1}{2}\,\eta'^2 \,-\,\frac{3}{2}\,\xi^2 \,-\,\frac{1}{|\eta|} \;&=\; c^{-2}h\;, \end{aligned} \tag{29}$$

where primes denote derivatives with respect to τ. The orbit in the limit $c \to 0$ exists if $h \to \infty$ such that $c^{-2}h$ has a finite limit. Elimination of η' from the first and the third equation of (29) yields

$$-\frac{3}{8}\,\xi^2 - \frac{1}{|\eta|} = c^{-2}h\;.$$

Since the above limit corresponds to $\xi \to 1$, $\eta \to \infty$ we obtain $c^{-2}h \to -\frac{3}{8}$, and the possible limiting orbits are given by

$$\eta = \frac{\pm 8/3}{1-\xi^2} \;\text{ for }\; |\xi| < 1\;. \tag{30}$$

In particular, the closest approach occurs for $\xi = 0$ which implies

$$|\eta_{\min}| = \frac{8}{3}\;. \tag{31}$$

In order to characterize a close encounter in coorbital motion it suffices to consider solutions of Hill's lunar problem for which the limit (27) exists, referred to as *non-oscillating orbits*. These orbits approximate the motion of coorbital satellites (described in rotating Jacobi coordinates) during a close encounter in the limit of small mass ratios $\epsilon \to 0$.

In Fig. 1 (overview) and Fig. 2 (details) a few typical non-oscillating orbits corresponding to various values of the impact parameter $c > 0$ are plotted. They all have their incoming branch in the first quadrant. Three types of orbits may be distinguished according to the value of c compared to the separating values

$$c_1 = 1.33611\,71883, \quad c_2 = 1.71877\,99380\;. \tag{32}$$

These types will be briefly discussed in the following, using the same nomenclature as for the types of coorbital motion introduced in Section 1.

Orbits of Type 1 are obtained if the impact parameter satisfies $c \in (0, c_1)$.

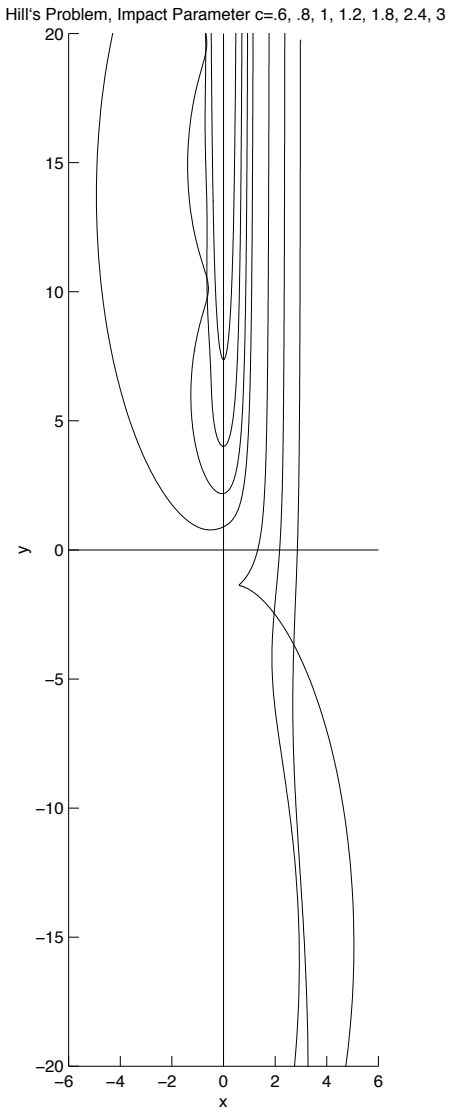

Fig. 1 The family of non-oscillating orbits in Hill's lunar problem. The incoming branch is in the first quadrant. From left to right, the values of the impact parameter are $c = 0.6$, 0.8, 1.0, 1.2 (Type 1), 1.8, 2.4, 3.0 (Type 2).

In the entire interval the orbit persistently escapes in the second quadrant as $t \to +\infty$. For sufficiently small values of c (in practice for $c < 0.8$) the orbit is well approximated by Equ. (30). In this interval the entire orbit depends continuously on the parameter c, and it is bounded away from the collision singularity at the origin. The limiting orbit for $c = c_1$ is asymptotic to a periodic orbit of Hill's problem with energy $h = -.375c_1^2$ and never escapes. Accordingly, the close encounters of coorbital motion corresponding to these values of c have the following properties:

- The leading body is the same before and after the close encounter.

- The upper and lower bodies exchange their roles such that the center of mass of the satellites remains at the same distance from m_0.

- For $c << 1$ (in practice $c < 0.8$) the minimum distance of the satellites during the close encounter is approximated by

$$D_{\min} = \epsilon^{1/3} R \cdot \frac{8}{3} c^{-2} = \frac{8}{3} R\epsilon\delta^{-2} , \tag{33}$$

as follows from (24), (28), (31), and (23). Here ϵ and δ are defined by (20) and (22), respectively.

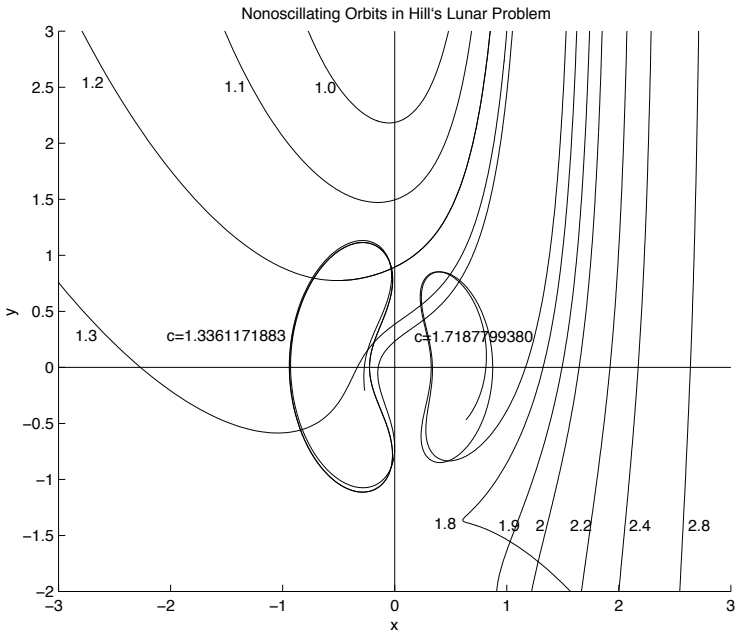

Fig. 2 Detail of Fig. 1. The limiting cases of orbits of Types 1 and 2 corresponding to $c = c_1$ and $c = c_2$, respectively (see Equ. (32)) are asymptotic to kidney-shaped periodic orbits of Hill's problem. Due to the hyperbolicity of these orbits (as fixed points of the Poincaré map) only a few revolutions can be traced numerically.

In the Saturnian ring system the satellites Janus and Epimetheus are currently on orbits of this kind. In Section 1 they were referred to as orbits of Type 1 or proper coorbital motion. Other notions are one-to-one resonance or horseshoe orbits, due to the horseshoe-like shape of the relative orbit in a rotating coordinate system. In Table 1 below the approximate orbital data of this pair of satellites are collected.

Close encounters of Type 2 are characterized by a sufficiently large value of the impact parameter c, more precisely by the condition $c > c_2$. Fig. 1 and Fig. 2 show that non-oscillating orbits of this type end in an escape in the fourth quadrant for $t \to \infty$. In the whole interval the entire orbit again depends continuously on c and is bounded away from the collision singularity at the origin. The limiting orbit for $c = c_2$ is again asymptotic to a periodic orbit of Hill's problem and never escapes. The close encounters of the corresponding coorbital motion have the properties

- The leading satellite becomes trailing and vice-versa.

- The upper satellite remains in the upper orbit, the lower satellite remains in the lower orbit.

Therefore, the lower (and faster) satellite merely passes the upper (and slower) one, without much interaction. In a circular configuration this *stable revolution* generally persists for a long time if $c > 3$. In the Saturnian ring system the F ring shepherds Pandora and Prometheus are an example of this situation (Table 1).

Non-oscillating orbits of Type 3 correspond to an impact parameter in the so-called transition region defined by $c \in (c_1, c_2)$. They depend on c in a very complicated, discontinuous way. The family has fractal structure with infinitely many orbits asymptotic to periodic orbits. Short intervals of continuous dependence on c are always followed by discontinuities. The orbits of the family cannot be bounded away from the collision singularity at the origin; the family contains infinitely many collision orbits. The orbits may generically end in an escape in the second, third or fourth quadrant (see Fig. 3). Therefore the corresponding close encounter in coorbital motion

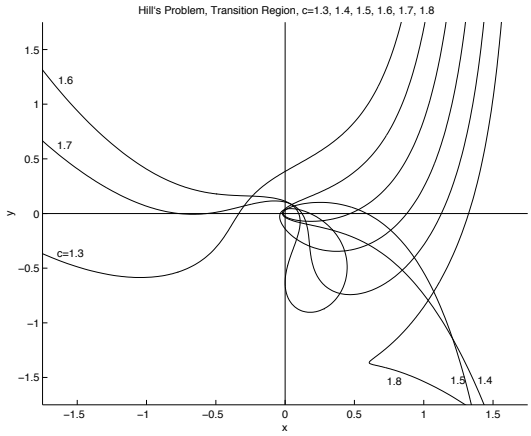

Fig. 3 Non-oscillating orbits from the transition region corresponding to the values $c = 1.4,\ 1.5,\ 1.6,\ 1.7$ of the impact parameter (from left to right on the incoming branch in the first quadrant). Every orbit involves close approaches with the singularity at the origin. The orbits corresponding to $c = 1.3$ and $c = 1.8$ outside the transition region are added for clarity.

may ultimately be of Type 1 or Type 2, but only after possible collisions of the satellites. Actual celestial bodies would thus not survive close encounters in the transition region.

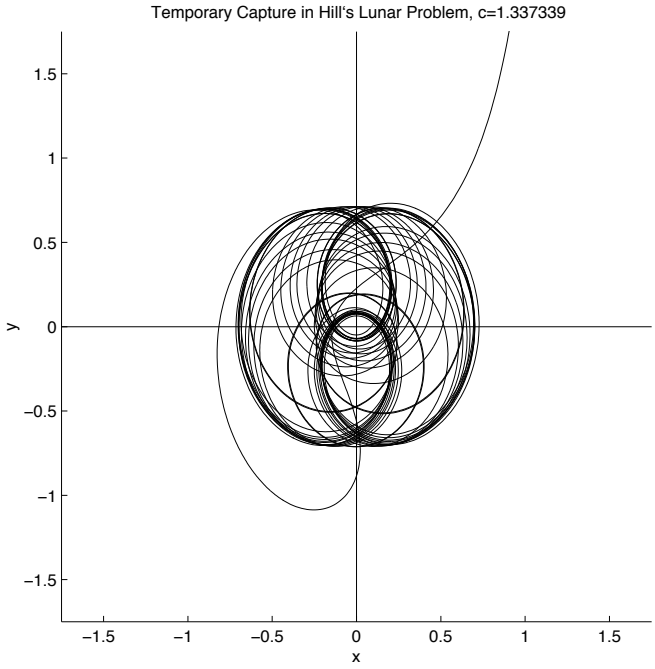

Fig. 4 Initial segment of the non-oscillating orbit with impact parameter $c = 1.337339$. The orbit is close to a quasiperiodic solution (torus); it escapes only after hundreds of revolutions (not shown).

An interesting phenomenon of non-oscillating orbits in the transition region is the existence of orbits close to quasiperiodic solutions (*tori*) of Hill's problem. These orbits carry out hundreds of revolutions about the origin before escaping (Fig. 4). In coorbital motion this corresponds to temporary capture between the two satellites in orbit about the central body. The experiments suggest that temporary capture can be achieved for an arbitrarily long time span. However, near-collisions between the satellites seem to be necessary.

In Table 1 below approximate orbital data of two actual coorbital pairs in the Saturnian ring system are listed. For the central body, Saturn, a normalized mass (mass times gravitational constant) of $m_0 = 3.8 \cdot 10^7$ km^3 sec^{-2} is assumed. The quantities ϵ, R_{12} and Δ, $\delta, c, D_{\min}$ are defined in (20), (21), (22), (23), (33), respectively. The periods of revolution T_k follow from the third Keplerian law,

$$T_k = 2\pi\sqrt{R_k^3/m_0}\,, \quad k = 1, 2\,,$$

and the synodic period $T_{\rm syn}$ (the time between two consecutive close encounters) is given by

$$T_{\rm syn} = \frac{1}{T_1^{-1} - T_2^{-1}} \doteq \frac{2}{3}\, T_1\, \delta^{-1} \,. \tag{34}$$

In the last line of Table 1 we give a measure $T_{\rm enc}$ of the duration of a close encounter of coorbital satellites. We say that the interaction begins when the trailing satellite "sees" the leading one in the tangential direction of its own orbit. The interaction is said to end in the inverse constellation. Simple geometry yields

$$T_{\rm enc} = \frac{L}{2\pi R_{12}} \cdot T_{\rm syn} \,,$$

where

$$L \doteq \sqrt{8 R_{12} \Delta}$$

is the length of the chord of the outer orbit which is tangential to the inner one. Combining these equations yields

$$T_{\rm enc} \doteq \frac{2\sqrt{2}}{3\pi}\, T_1 \cdot \delta^{-1/2} \,. \tag{35}$$

	Type 1 Janus-Epimetheus	Type 2 Pandora-Prometheus
ϵ	$8 \cdot 10^{-9}$	$1.64 \cdot 10^{-9}$
R_{12}	151 460 km	140 270 km
Δ	50 km	2350 km
δ	0.00033	0.0167
c	0.165	14.2
$D_{\rm min}$	29700 km	2350 km
T_1, T_2	16.68 h	14.7 h, 15.1 h
$T_{\rm syn}$	1404 days	24.8 days
$T_{\rm enc}$	275 h = 16.5 revol.	2.3 revolutions

Table 1

4 Long-Term Evolution

The long-term evolution of a coorbital pair is determined by the close encounters between the satellites. It strongly depends on the successive types of the close encounters as they

are discussed in Section 3. We will first define coordinate systems appropriate for describing all phases of coorbital motion: the close encounters, the intervening time intervals of perturbed Kepler motions, and the intervals of temporary capture between the satellites.

The starting point is the system of Jacobi coordinates R, D and their canonically conjugated momenta P_R, P_D (see Equs. (10), (13)), resulting in the Hamiltonian (14). In order to describe the relative motion of m_2 with respect to m_1 in a simple way we introduce a rotating and pulsating coordinate system. One way to do this is to measure the relative coordinate D with respect to the center-of-mass coordinate R, i.e. to introduce the complex ratio

$$Q := D/R \tag{36}$$

as a new coordinate. In order to carry out this transformation within the canonical formalism we augment (36) by the identical transformation $S := R$, thus denoting the new (unchanged) center-of-mass coordinate by S. Hence, the coordinate transformation becomes

$$\begin{aligned} R &= S \\ D &= S \cdot Q \; . \end{aligned} \tag{37}$$

Following the procedures of Section 2.1 we obtain the canonically conjugated momenta P_S, P_Q from the generating function

$$W = \frac{1}{2} \left(S \, \overline{P}_R + \overline{S} \, P_R + SQ \, \overline{P}_D + \overline{S} \, \overline{Q} \, P_D \right)$$

as

$$P_S = 2 \, \frac{\partial W}{\partial \overline{S}} \, , \quad P_Q = 2 \, \frac{\partial W}{\partial \overline{Q}} \, .$$

Solving these equations for the old momenta yields

$$P_R = P_S - \frac{\overline{Q}}{\overline{S}} \, P_Q, \quad P_D = \frac{P_Q}{\overline{S}} \, . \tag{38}$$

Substituting (37), (38) into the Hamiltonian (14) yields

$$\begin{aligned} H = \; & \frac{1}{2|S|^2} \left(\left(\frac{1}{m_0} + \frac{1}{m_1 + m_2} \right) \left| \overline{S} \, P_S - \overline{Q} \, P_Q \right|^2 \right. \\ & \left. + \left(\frac{1}{m_0} + \frac{1}{m_2} \right) \left| P_Q \right|^2 \right) \\ & - \frac{1}{|S|} \left(\frac{m_0 m_1}{|1 - \mu_2 Q|} + \frac{m_0 m_2}{|1 + \mu_1 Q|} + \frac{m_1 m_2}{|Q|} \right) . \end{aligned} \tag{39}$$

Obviously, this coordinate system generates singularities when the center of mass of m_1 and m_2 passes through the origin, $S = 0$. This cannot happen during a close encounter of m_1, m_2; however, it may happen if the satellites occupy nearly opposite positions on their orbits about m_0.

The following consideration involving two small satellites moving on independent circular Keplerian orbits

$$z_k = r_k\, e^{i\omega_k t},\ (k=1,2),\ \omega_1^2 r_1^3 = \omega_2^2 r_2^3$$

will indicate the behavior of Q near this singularity. Equs. (10), (37) imply

$$Q = \frac{z_2 - z_1}{\mu_2 z_2 + \mu_1 z_1}\,.$$

Simplifying by z_1 reveals the orbit of the variable Q as the image of the circle $z = z_2/z_1 = r_2/r_1 \cdot e^{i(\omega_2-\omega_1)t}$ under a Möbius transformation, i.e. again a circle. If S passes through the origin, Q passes through infinity, i.e. its orbit is a straight line (a circle with infinite radius).

On the other hand, during a close encounter of m_1 and m_2 the coordinate S nearly travels on a Keplerian orbit; therefore Q describes the relative motion of z_2 with respect to z_1 in the rotating-pulsating coordinates defined by the Kepler motion of S. Hence the quotient Q behaves as Hill's coordinates of Section 3 in every close encounter (compare Fig. 1 with Fig. 6 below). These segments are connected by near-circular arcs (see Fig. 5 below). In the variable Q the types of motion discussed earlier can easily be distinguished:

Type 1: Proper coorbital motion is characterized by a long sequence of close encounters, each one characterized by a single near-perpendi-cular intersection with the imaginary axis. The orbit of Q has the shape of a horseshoe. For $m_1 = m_2$ the connecting near-circular arcs may pass through the right or the left half-plane and seem to change in a chaotic way.

Type 2: Stable revolution is characterized by an orbit of Q consisting of perturbed circles without intersections with the imaginary axis.

Type 3: Temporary capture: Q enters the vicinity of the origin and stays there for a long time.

The Hamiltonian (39) may finally be regularized in two steps: By applying Levi-Civita's transformation to the variable Q the collisions between m_1 and m_2 are regularized. With q, P_q being the new coordinates and momenta, and τ_1, K_1 being the new time and Hamiltonian, we transform

$$Q = q^2, \quad P_Q = \frac{P_q}{2\overline{q}}\,, \quad dt = |q|^2\, d\tau_1 \quad K_1 = |q|^2(H-h)\,, \tag{40}$$

where h is the value of the Hamiltonian on the orbit under consideration.

The second step is to transform the variable S in a similar way:

$$S = s^2, \quad P_S = \frac{P_s}{2\overline{s}}\,, \quad d\tau = |s|^4\, d\tau_1, \quad K = |s|^4\, K_1\,. \tag{41}$$

Here s, P_s, τ, K are again the new coordinates, new momenta, independent variable, and Hamiltonian. In addition to being analogous to the transformation (40), (41) "linearizes"

the unperturbed equations of motion of the center of mass [10] and introduces the true anomaly of this motion as a new independent variable. These variables were used by Scheibner [7] in the elliptic restricted three-body problem. The transformed Hamiltonian becomes

$$\begin{aligned} K = \; & \frac{1}{8}\left(\frac{1}{m_0}+\frac{1}{m_1+m_2}\right)|q|^2\,|\overline{s}\,P_s-\overline{q}\,P_q|^2+\frac{1}{8}\left(\frac{1}{m_1}+\frac{1}{m_2}\right)|P_q|^2 \\ & -|s|^2\left(\frac{m_0m_1\,|q|^2}{|1-\mu_2q^2|}+\frac{m_0m_2\,|q|^2}{|1+\mu_1\,q^2|}+m_1m_2\right)-h\,|q|^2\,|s|^4\;, \end{aligned} \tag{42}$$

and the equations of motion are

$$\begin{aligned} \frac{dq}{d\tau} &= 2\,\frac{\partial K}{\overline{P}_q}\;, \quad \frac{dP_q}{d\tau}=-2\,\frac{\partial K}{\partial\overline{q}} \\ \frac{ds}{d\tau} &= 2\,\frac{\partial K}{\overline{P}_s}\;, \quad \frac{dP_s}{d\tau}=-2\,\frac{\partial K}{\partial\overline{s}}\;, \quad \frac{dt}{d\tau}=|qs^2|^2\;. \end{aligned} \tag{43}$$

In the types of motion and time intervals considered in this work the collisions of the satellites with m_0 are excluded (i.e. the denominators in (42) are > 0); hence Equ. (43) are expected to be well suited for studying planar coorbital motion.

5 Results and Conclusions

For generating orbits of coorbital pairs we use roughly opposite initial positions and circular initial velocities. The initial positions will be defined according to Equ. (8), i.e. by

$$x_1 = x_0 + z_1, \quad x_2 = x_0 + z_2\;,$$

where

$$x_0 = -\frac{m_1z_1+m_2z_2}{M}\;, \quad M = m_0+m_1+m_2\;.$$

Nearly opposite values for z_1 and z_2, e.g.

$$z_2 = -1, \quad z_1 = 1+\delta, \quad |\delta| << 1 \tag{44}$$

were chosen in all the experiments. According to Kepler's laws the circular initial velocities are given by the complex momenta

$$p_1 = im_1\sqrt{\frac{M}{x_1}}\;, \quad p_2 = -im_2\sqrt{\frac{M}{-x_2}}\;. \tag{45}$$

A large number of orbits of coorbital pairs of all three types were computed numerically, using initial data according to (44), (45) with δ and ϵ (Equ. (20)) in the range $10^{-1}\ldots10^{-3}$. For sufficiently small mass ratios ϵ motion of Type 1 is obtained initially if $|\delta| < c\cdot\epsilon^{1/3}$ and $c < 1.33$. In this way it was possible to observe a sufficient number of

revolutions of coorbital motion as well as the process of its decay. The representation of the relative motion of m_2 with respect to m_1 in rotating-pulsating coordinates Q (Equs (36), (10)) proves to be an excellent means for visualizing the long-term behavior of the coorbital pair.

In all the experiments it was possible to continue the computation until the coorbital pair broke up. Similar results were obtained by G. Auner and R. Dvorak [1] in a numerical study with small mass ratios $\epsilon < 10^{-4}$. In most of their experiments with $\delta > 0.7 \cdot \epsilon^{1/3}$ break-up of the coorbital pair within 10′000 close encounters was observed. Therefore it may be conjectured that coorbital pairs have a *finite lifetime* (which may be very long, though).

We restrict ourselves to visualize the long-term evolution and decay of coorbital motion by means of a typical example.

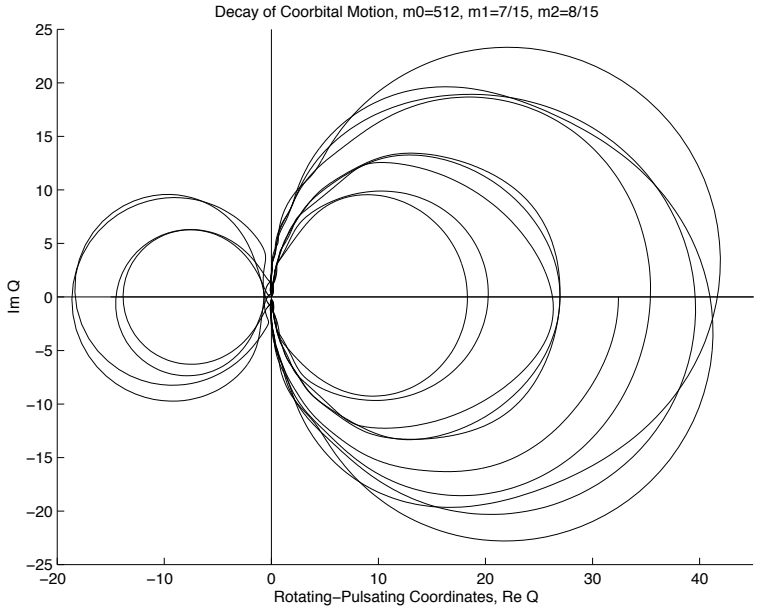

Fig. 5 Relative motion in a coorbital pair, shown in rotating-pulsating coordinates. Masses: $m_0 = 512$, $m_1 = 7/15$, $m_2 = 8/15$. Circular initial positions: $z_1 = -1$, $z_2 = 1.01$. The pair breaks up after 10 close encounters; 4 more close encounters of the subsequent Type-2 motion are shown.

Figure 5, giving an overall view of the relative motion in rotating-pulsating coordinates, clearly displays 10 near-circular connecting arcs representing 10 intervals of weakly perturbed Kepler motion between 10 close encounters. These circles are slightly deformed since the Kepler orbits have small eccentricities. The succession of connecting arcs is generally non-monotonic, in fact is seems to be totally irregular and impredictable. After the break-up of the coorbital pair the motion of this system transforms into Type-2 motion (stable revolution); 4 more close encounters are shown in the figure.

The behavior near the close encounters is seen in Fig. 6, a mere close-up view of the neighbourhood of the origin of Fig. 5. The 10 close encounters of Type-1 motion are represented by the U-shaped branches entering the picture from above and from below. These encounters slowly "deteriorate" in an irregular but systematic way: the minimum distance decreases until the pair breaks up in a near-collision. The branches on the left side of the figure represent the first 4 close encounters in the subsequent Type-2 motion.

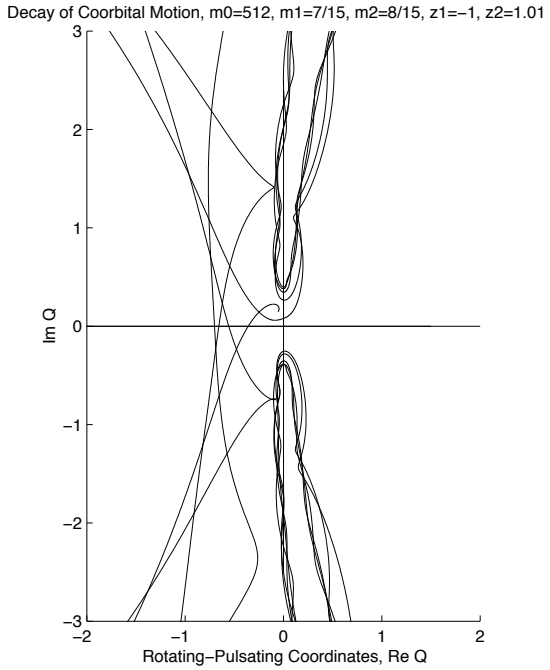

Fig. 6 Detail of Fig. 5 (neighbourhood of the origin). The coorbital pair breaks up with the tenth close encounter.

Finally, we mention a surprising observation concerning temporary capture between two satellites in nearly identical orbits about a central body. In Section 3 (Figure 4) we gave an example of long temporary capture in Hill's lunar problem, which is the limiting case $\epsilon \to 0$ of coorbital motion. Our experiments suggest that the phenomenon of temporary capture, between coorbital satellites possibly for arbitrarily long times, exists also for finite mass ratios $\epsilon > 0$. Fig. 7 shows the initial section of an orbit corresponding to $\epsilon = 1/343$ which remains in bound state for more than 100 revolutions. Similar orbits have been found for mass ratios as large as $\epsilon = 0.1$. Note the striking similarity between Fig. 7 and Fig. 4.

The analysis of some of the phenomena of this section by means of appropriate surfaces-of-section is deferred to a later paper.

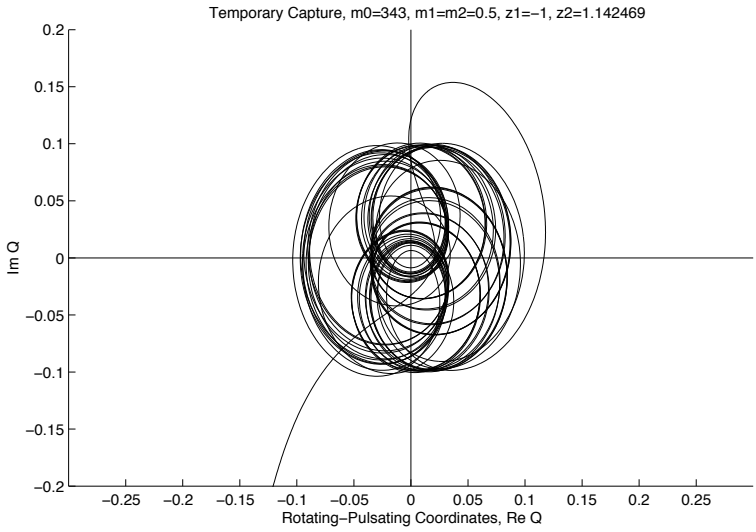

Fig. 7 Temporary capture between two satellites in orbit. Masses: $m_0 = 343$, $m_1 = m_2 = 1/2$. Circular initial positions: $z_1 = -1$, $z_2 = 1.142469$. The bound state breaks up only after more than 100 revolutions (not shown here). Note the similarity with Fig. 4.

References

[1] Auner, G. and Dvorak, R.: *Close planetary orbits and their cosmological importance.* In: J. Hagel, M. Cunha, R. Dvorak (eds), Perturbation Theory and Chaos in Nonlinear Dynamics with Emphasis to Celestial Mechanics. Universität Wien, 1-17, (1995).

[2] Dermott, S.F. and Murray, C.D.: The dynamics of tadpole and horseshoe orbits, I, II. *Icarus*, **48**, 1-22, (1981).

[3] Gruntz, D. and Waldvogel, J.: *Orbits in the planar three-body problem.* In: W. Gander, J. Hrebicek (eds), Solving Problems in Scientific Computing using Maple and Matlab. Springer-Verlag, 37-57, (1991).

[4] Hénon, M. and Petit, J.M.: Series expansions for encounter-type solutions of Hill's problem. *Celest. Mech.*, **38**, 67-100, (1986).

[5] Levi-Civita, T.: Sur la régularisation du problème des trois corps. *Acta Math.*, **42**, 99-144, (1920).

[6] Petit, J.M. and Hénon, M.: Satellite encounters. *Icarus*, **66**, 536-555, (1986).

[7] Scheibner, W.: Satz aus der Störungstheorie. *J. Reine Angew. Math.*, **65**, 291, (1866).

[8] Siegel, C.L., and Moser, J.: *Lectures on Celestial Mechanics.* Springer-Verlag, 290 pp. , (1971).

[9] Spirig, F. and Waldvogel, J.: *The three-body problem with two small masses: A singular-perturbation approach to the problem of Saturn's coorbiting satellites.* In: V. Szebehely (ed), Stability of the Solar System and its Minor Natural and Artificial Bodies. Reidel, 53-63, (1985).

[10] Stiefel, E. and Scheifele, G.: *Linear and Regular Celestial Mechanics.* Springer-Verlag, 301 pp., (1971).

[11] Waldvogel, J.: A new regularization of the planar problem of three bodies. *Celest. Mech.*, **6**, 221-231, (1972).

[12] Waldvogel, J. and Spirig, F.: *Chaotic motion in Hill's lunar problem.* In: A.E. Roy and B.A. Steves (eds), From Newton to Chaos: Modern Techniques for Understanding and Coping with Chaos in N-Body Dynamical Systems. Plenum Press, 217-230, (1995).

Research Reports

No.	Authors	Title
98-05	J. Waldvogel	Long-Term Evolution of Coorbital Motion
98-04	R. Sperb	An alternative to Ewald sums, Part 2: The Coulomb potential in a periodic system
98-03	R. Sperb	The Coulomb energy for dense periodic systems
98-02	J.M. Melenk	On n-widths for Elliptic Problems
98-01	M. Feistauer, C. Schwab	Coupling of an Interior Navier–Stokes Problem with an Exterior Oseen Problem
97-20	R.L. Actis, B.A. Szabo, C. Schwab	Hierarchic Models for Laminated Plates and Shells
97-19	C. Schwab, M. Suri	Mixed *hp* Finite Element Methods for Stokes and Non-Newtonian Flow
97-18	K. Gerdes, D. Schötzau	*hp* FEM for incompressible fluid flow - stable and stabilized
97-17	L. Demkowicz, K. Gerdes, C. Schwab, A. Bajer, T. Walsh	HP90: A general & flexible Fortran 90 *hp*-FE code
97-16	R. Jeltsch, P. Klingenstein	Error Estimators for the Position of Discontinuities in Hyperbolic Conservation Laws with Source Terms which are solved using Operator Splitting
97-15	C. Lage, C. Schwab	Wavelet Galerkin Algorithms for Boundary Integral Equations
97-14	D. Schötzau, C. Schwab, R. Stenberg	Mixed *hp* - FEM on anisotropic meshes II: Hanging nodes and tensor products of boundary layer meshes
97-13	J. Maurer	The Method of Transport for mixed hyperbolic - parabolic systems
97-12	M. Fey, R. Jeltsch, J. Maurer, A.-T. Morel	The method of transport for nonlinear systems of hyperbolic conservation laws in several space dimensions
97-11	K. Gerdes	A summary of infinite element formulations for exterior Helmholtz problems
97-10	R. Jeltsch, R.A. Renaut, J.H. Smit	An Accuracy Barrier for Stable Three-Time-Level Difference Schemes for Hyperbolic Equations
97-09	K. Gerdes, A.M. Matache, C. Schwab	Analysis of membrane locking in *hp* FEM for a cylindrical shell
97-08	T. Gutzmer	Error Estimates for Reconstruction using Thin Plate Spline Interpolants